Supporting Information

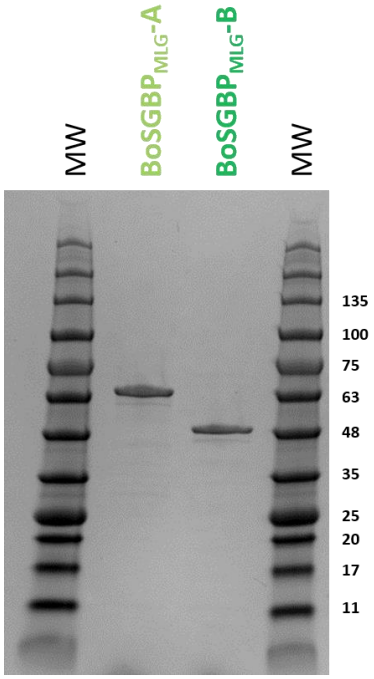

Figure S1. Recombinant proteins. SDS-PAGE of purified SGBPs with molecular weight (MW) ladders on either side; ladder band sizes are on the right in kilodaltons (kDa). The calculated expected molecular weights are 62.5 kDa for BoSGBP$_{MLG}$-A and 45.5 kDa for BoSGBP$_{MLG}$-B.

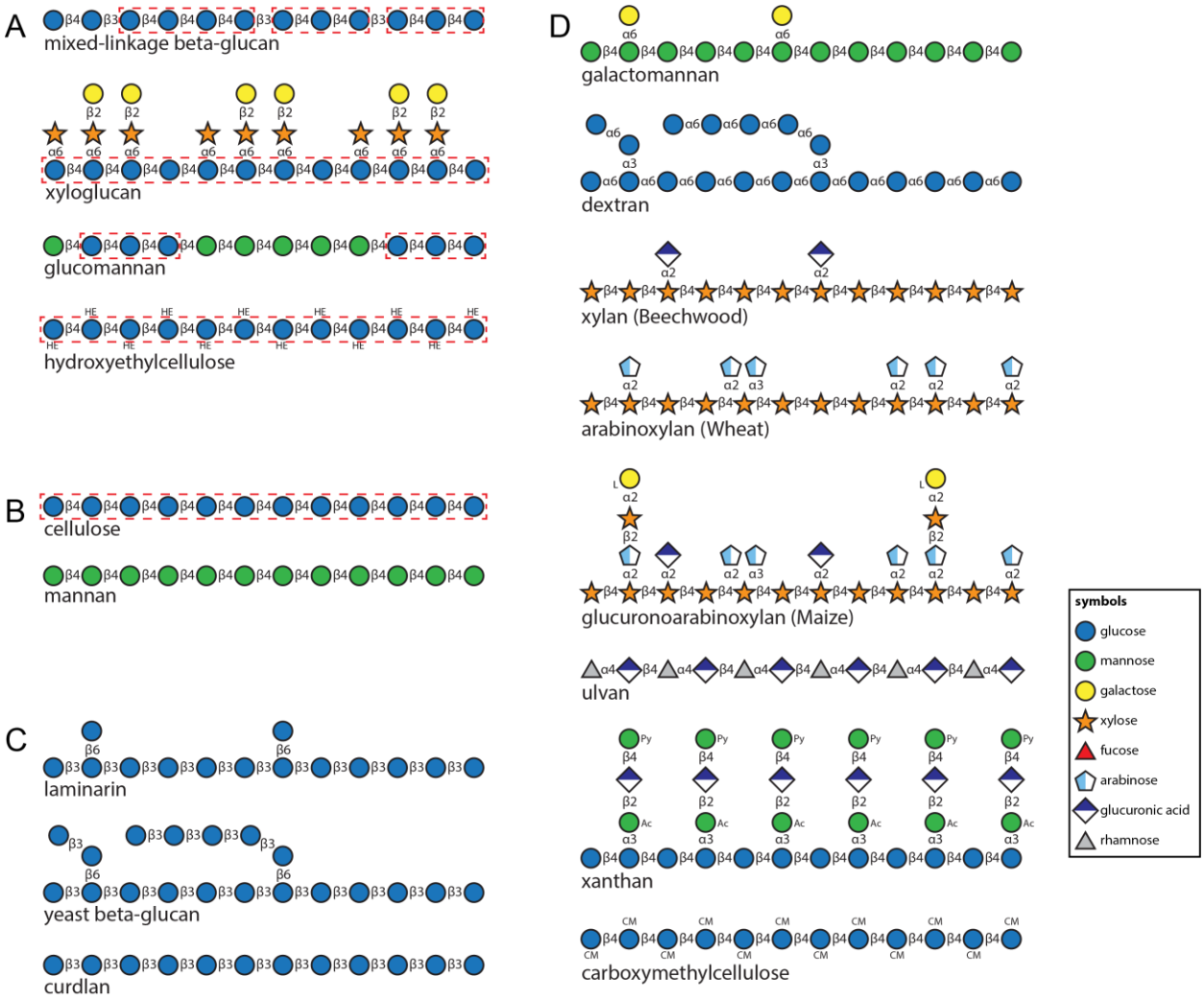

Figure S2. Structures of polysaccharides. (A) Polysaccharides that BoSGBP$_{MLG}$-A and BoSGBP$_{MLG}$-B bind (B) Insoluble polysaccharides. (C) Other β-glucans tested that BoSGBP$_{MLG}$-A and BoSGBP$_{MLG}$-B did not bind. (D) Other polysaccharides tested that BoSGBP$_{MLG}$-A and BoSGBP$_{MLG}$-B did not bind. The dashed red boxes highlight the β(1,4)-linked glucose units in the backbone, which are common to all polysaccharides that BoSGBP$_{MLG}$-A and BoSGBP$_{MLG}$-B bind.

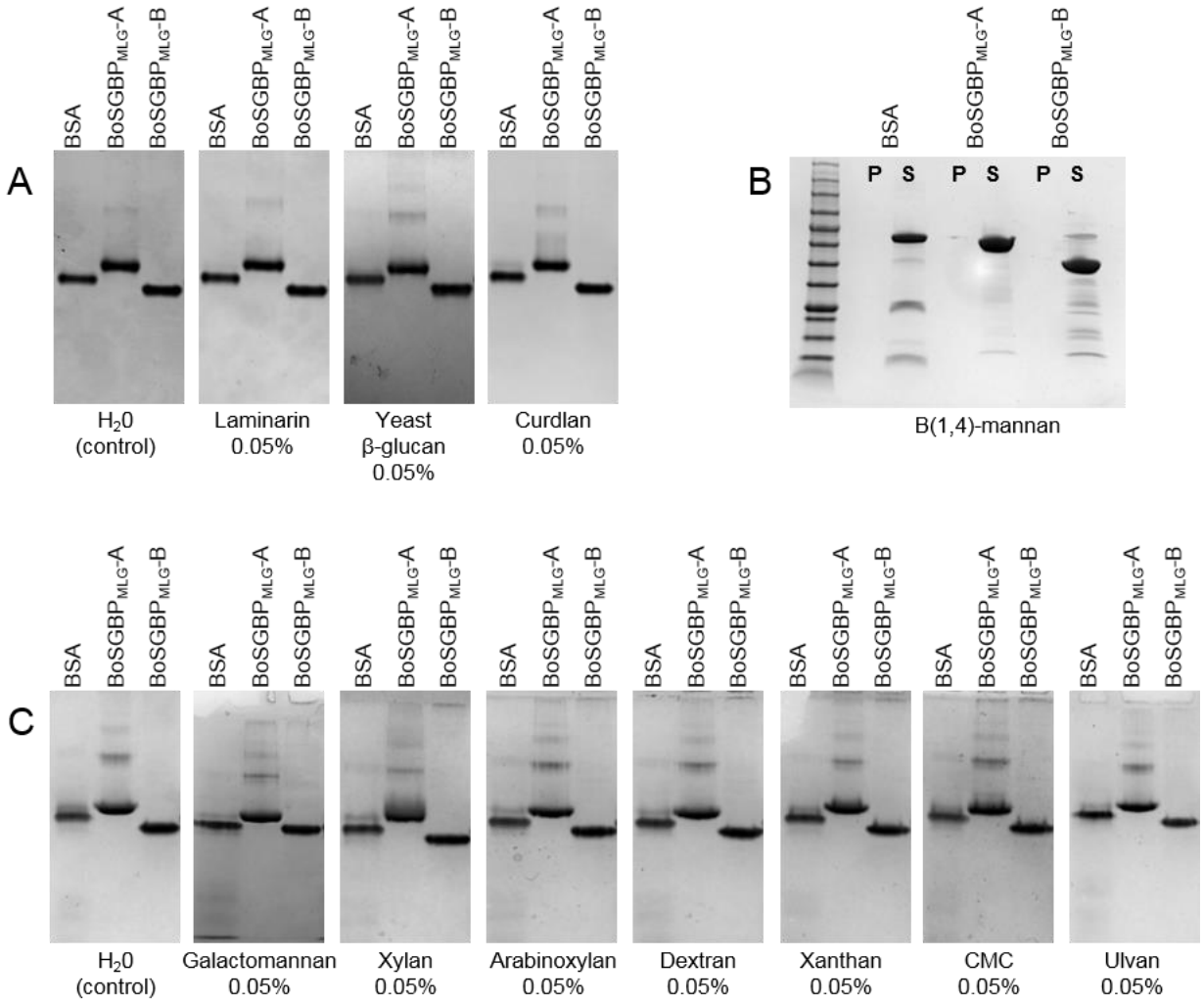

Figure S3. BoSGBP$_{MLG}$-A and BoSGBP$_{MLG}$-B non-binding polysaccharides. (A) Affinity electrophoresis gels against β(1,3)-glucans. (B) SDS-PAGE of pull-down assay against insoluble mannan. (C) Affinity electrophoresis gels against various other polysaccharides.

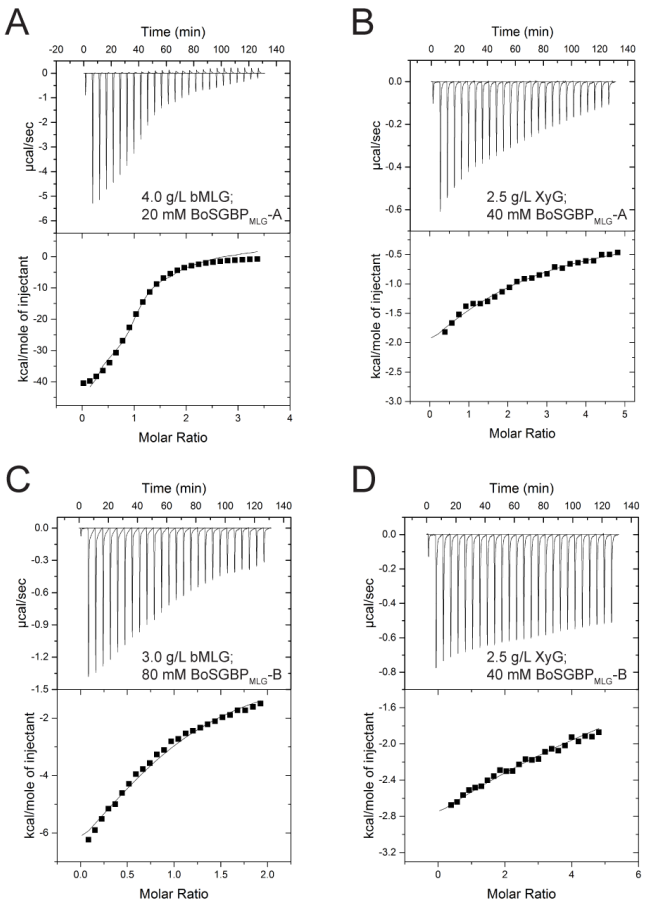

Figure S4. Representative isothermal titration calorimetry (ITC) results for BoSGBP$_{MLG}$-A and BoSGBP$_{MLG}$-B with bMLG and XyG. All titrations were performed in 50 mM Sodium Phosphate pH 7.0 with the exception of BoSGBP$_{MLG}$-B with bMLG (performed in 10 mM HEPES pH 7.0) and at 25 °C. In each case, the upper graph shows the raw heat signal for the 10 µL injections of carbohydrate into protein; the bottom graph shows the integrated heats and, where appropriate, fits to a 1:1 binding model. Concentrations of the protein and glycan are indicated in the figure. (A) BoSGBP$_{MLG}$-A with bMLG, (B) BoSGBP$_{MLG}$-A with XyG, (C) BoSGBP$_{MLG}$-B with bMLG, (D) BoSGBP$_{MLG}$-B with XyG.

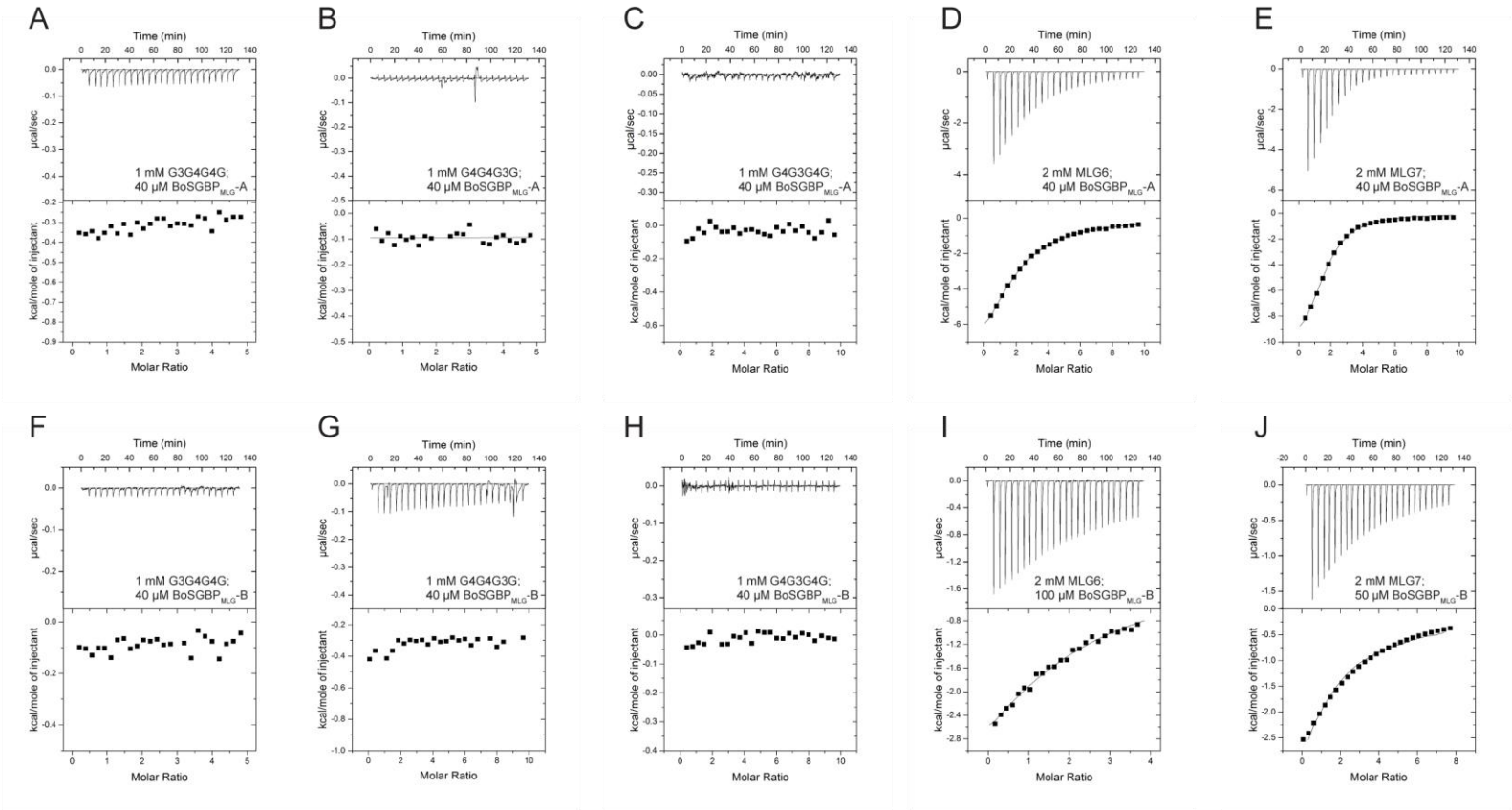

Figure S5. Representative ITC results for BoSGBP$_{MLG}$-A and BoSGBP$_{MLG}$-B with MLG oligosaccharides. All titrations were performed in 50 mM Sodium Phosphate pH 7.0 and at 25 °C. In each case, the upper graph shows the raw heat signal for the 10 µL injections of carbohydrate into protein; the bottom graph shows the integrated heats and, where appropriate, fits to a 1:1 binding model. Concentrations of the protein and glycan are indicated in the figure. (A) BoSGBP$_{MLG}$-A with G3G4G4G, (B) BoSGBP$_{MLG}$-A with G4G4G3G, (C) BoSGBP$_{MLG}$-A with G4G3G4G, (D) BoSGBP$_{MLG}$-A with MLG6, (E) BoSGBP$_{MLG}$-A with MLG7, (F) BoSGBP$_{MLG}$-B with G3G4G4G, (G) BoSGBP$_{MLG}$-B with G4G4G3G, (H) BoSGBP$_{MLG}$-B with G4G3G4G, (I) BoSGBP$_{MLG}$-B with MLG6, (J) BoSGBP$_{MLG}$-B with MLG7.

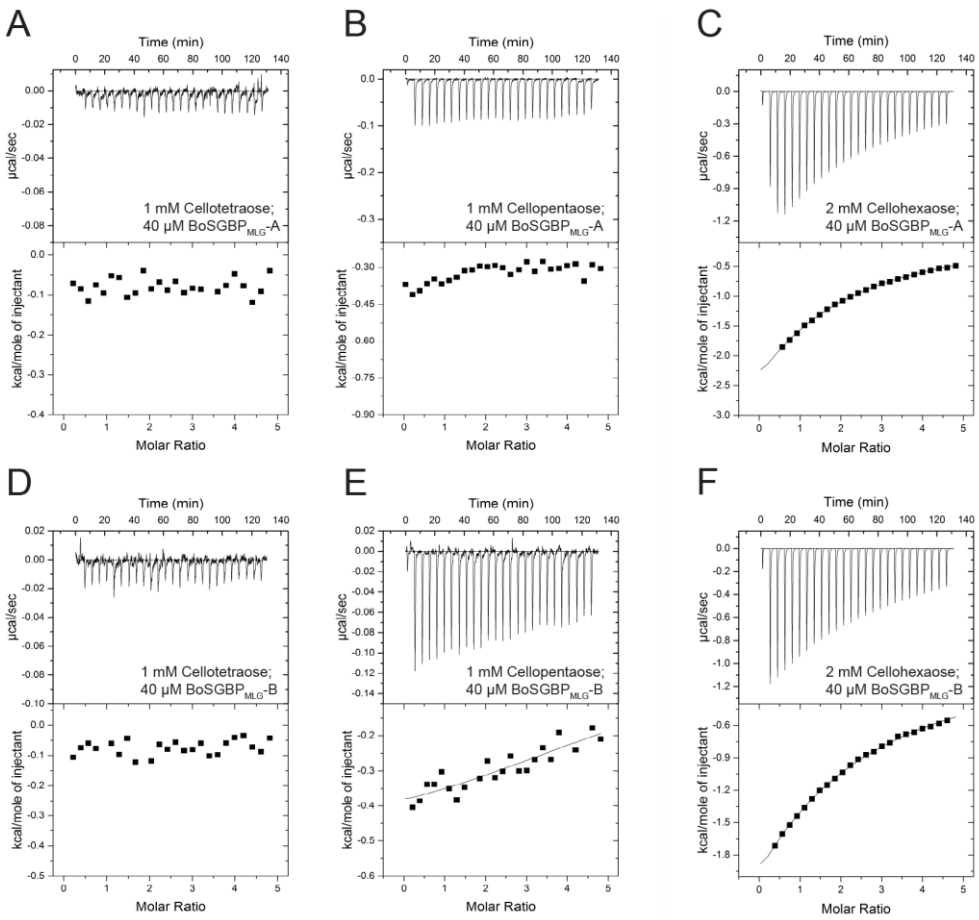

Figure S6. Representative ITC results for BoSGBP$_{MLG}$-A and BoSGBP$_{MLG}$-B with cellooligosaccharides. All titrations were performed in 50 mM Sodium Phosphate pH 7.0 and at 25 °C. In each case, the upper graph shows the raw heat signal for the 10 µL injections of carbohydrate into protein; the bottom graph shows the integrated heats and, where appropriate, fits to a 1:1 binding model. Concentrations of the protein and glycan are indicated in the figure. (A) BoSGBP$_{MLG}$-A with cellotetraose, (B) BoSGBP$_{MLG}$-A with cellopentaose, (C) BoSGBP$_{MLG}$-A with cellohexaose, (D) BoSGBP$_{MLG}$-B with cellotetraose, (E) BoSGBP$_{MLG}$-B with cellopentaose (F) BoSGBP$_{MLG}$-B with cellohexaose.

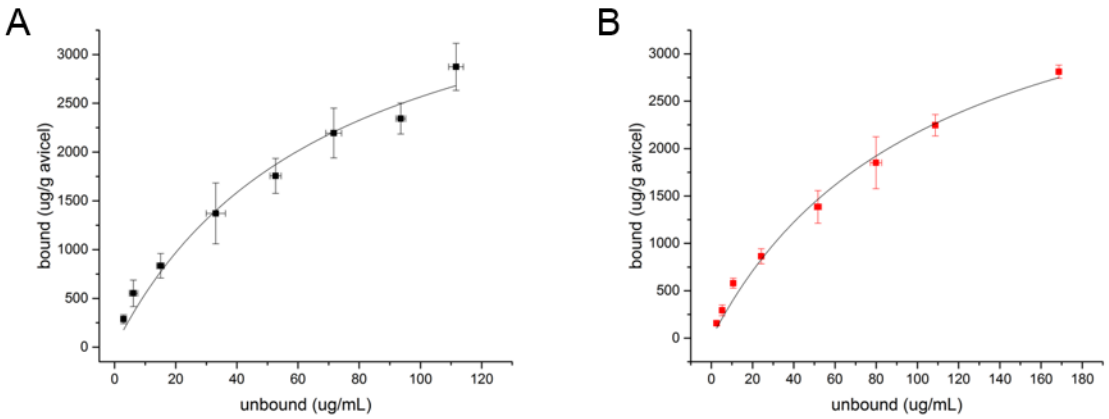

Figure S7. Avicel depletion isotherm for (A) GFP-BoSGBP$_{MLG}$-A and (B) GFP-BoSGBP$_{MLG}$-B. The dissociation constants (K_d) extracted from curve fitting (see methods for details) are 49.1 ± 13.1 µM and 117.4 ± 21.0 µM for GFP-BoSGBP$_{MLG}$-A and GFP-BoSGBP$_{MLG}$-B, respectively. Corresponding association constants (K_a) are 2.04 (± 0.54) x 10^4 M^{-1} and 8.52 (± 1.50) x 10^3 M^{-1} respectively for GFP-BoSGBP$_{MLG}$-A and GFP-BoSGBP$_{MLG}$-B.

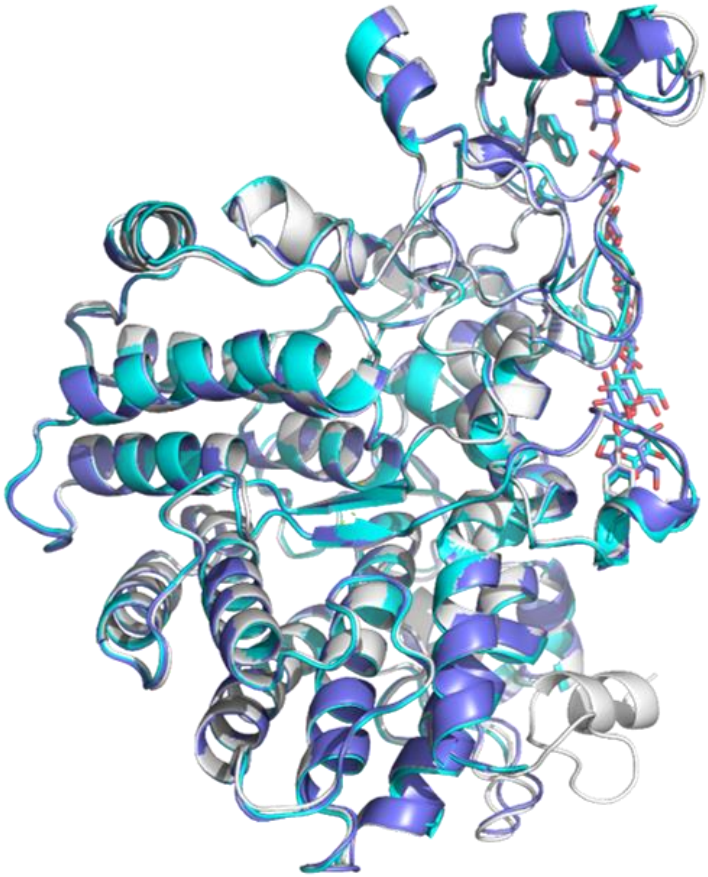

Figure S8. Overlay of $BoSGBP_{MLG}$-A secondary structures. Unliganded structure in white, cellohexaose complex in cyan, and MLG7 complex in slate show no major conformational differences with each other. Electron density for an extra 19 N-terminal residues were resolved only in the high resolution (1.50 Å, 6E60) unliganded structure, a portion of which folds into a short α-helix. Because this extra resolved density is involved in crystal contact with the binding platform of a symmetry-related molecule not present in either of the complex structures (6DMF and 6E61), includes a part of the non-native recombinant sequence, and is a part of the sequence that is believed to form a disordered linker between the globular fold of the protein and the phospholipid to which it is anchored, we interpret this extra ordered structure (in particular the α-helix) to be a crystal artifact.

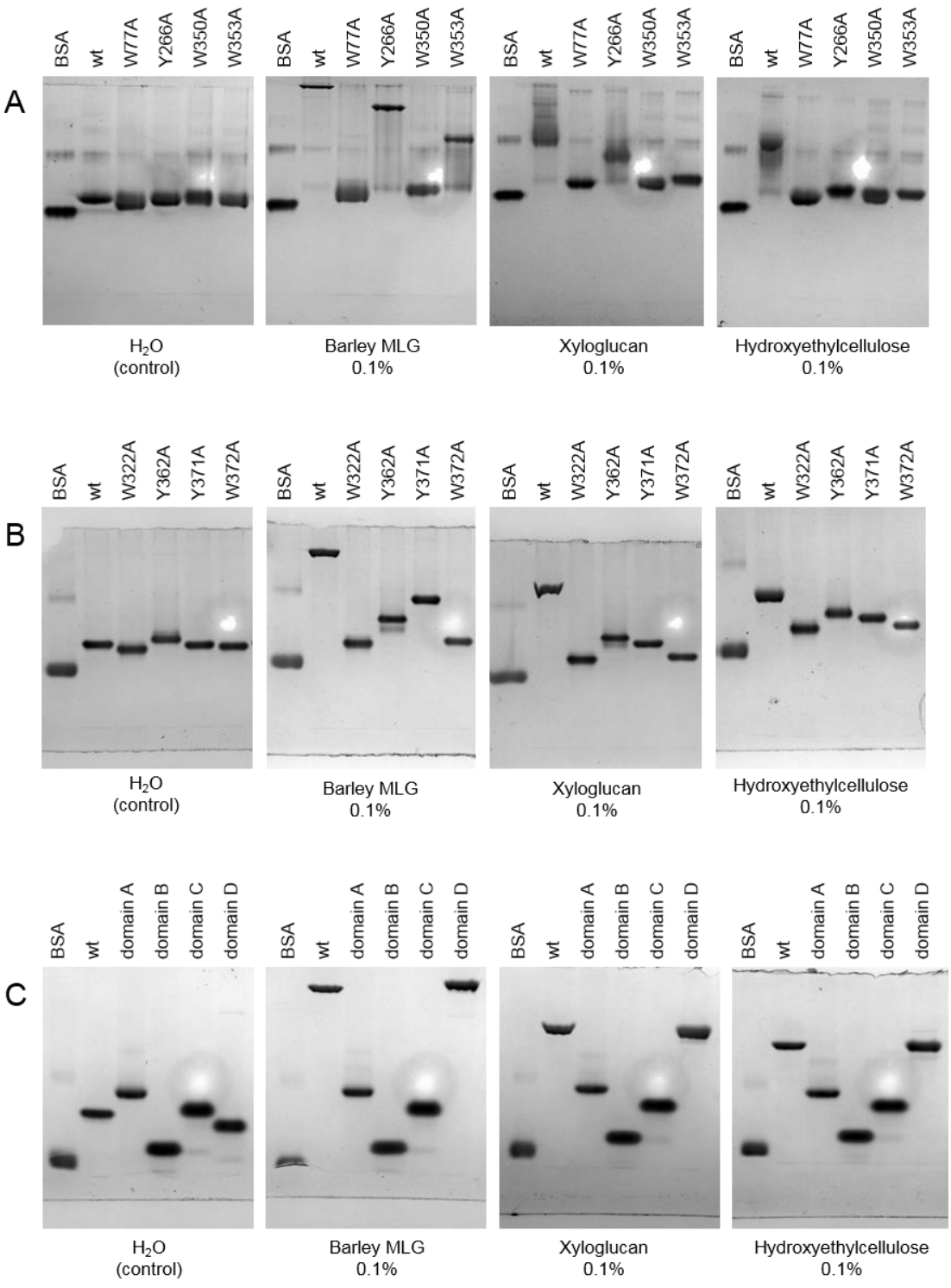

Figure S9. Affinity electrophoresis gels of site directed mutants and domain dissections on various polysaccharides. (A) BoSGBP$_{MLG}$-A binding platform site-directed mutants, (B) BoSGBP$_{MLG}$-B binding platform site-directed mutants, (C) BoSGBP$_{MLG}$-B domains. To facilitate comparison, the water and bMLG gels in panel A is identical to that shown in Fig. 3F, while those in panels B and C are identical to those shown in Fig. 4E.

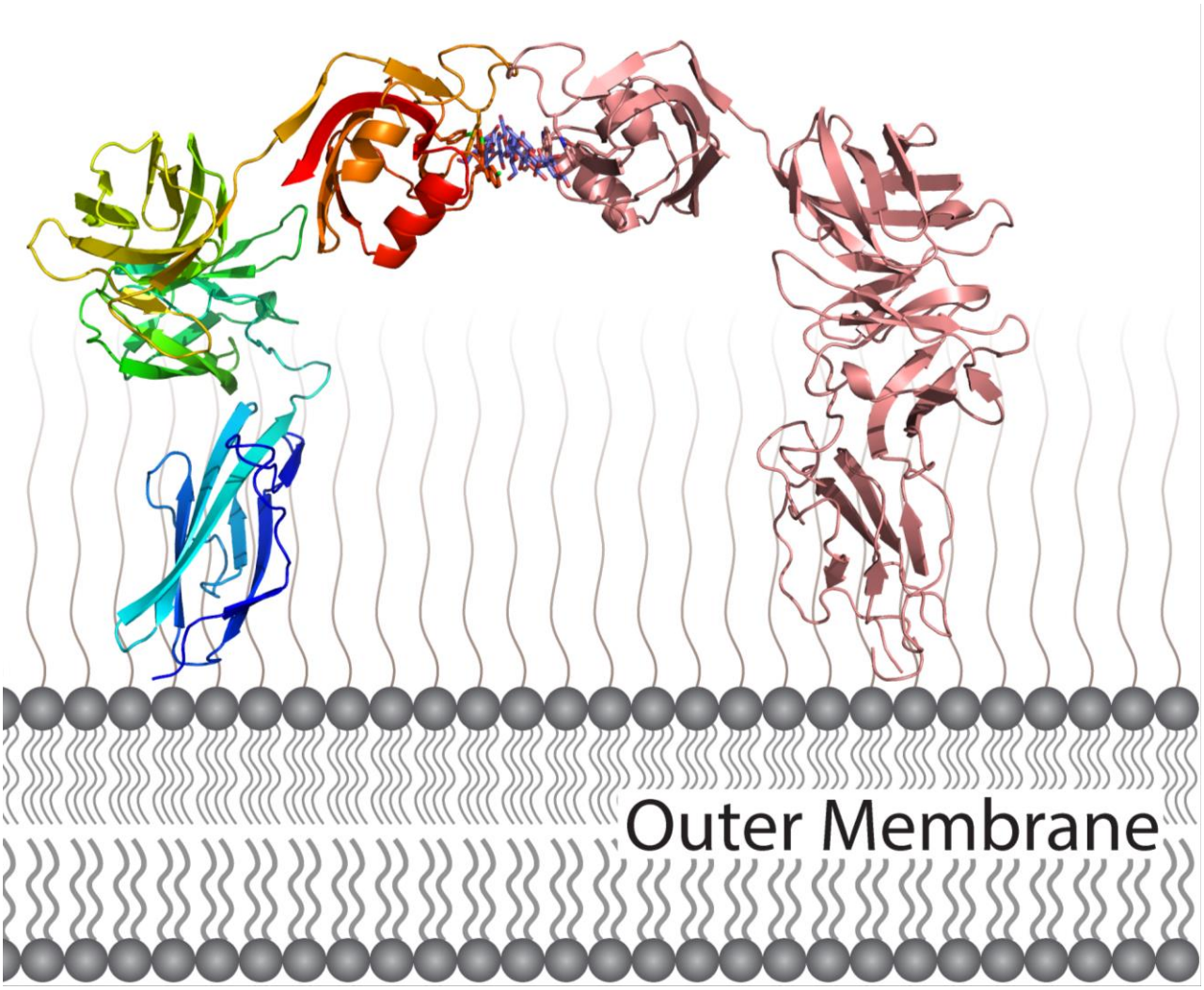

Figure S10. Representation of a single MLG7 ligand bound by two molecules of $BoSGBP_{MLG}$-B at the cell surface, based on crystallographic data (PDB ID 6E9B). The molecule on the left is color ramped from blue (N-terminus) to red (C-terminus), the symmetry related molecule on the right is colored salmon and the shared MLG7 ligand in the middle is colored slate. An analogous binding mode was observed for a cellohexaose complex (PDB ID 6E57).

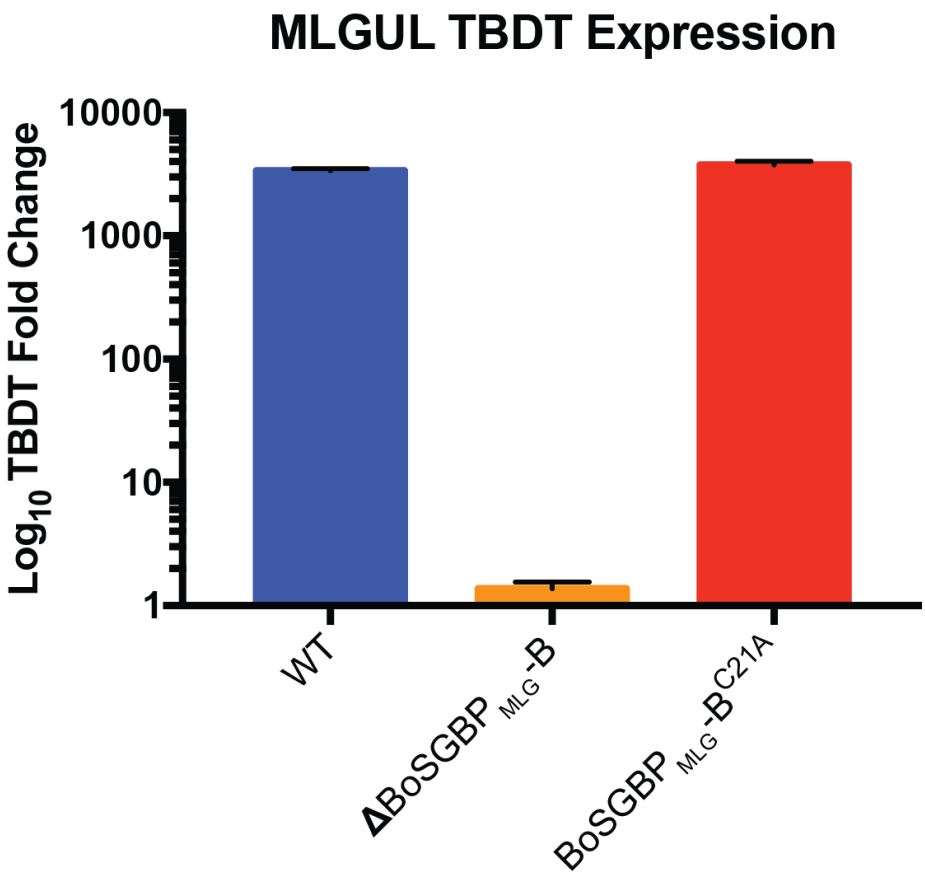

Figure S11. Transcriptional analysis of MLGUL TBDT in *BoSGBP$_{MLG}$-B* mutants. Fold change transcriptional response of the MLGUL TBDT from cells grown on MLG (5 mg/mL) vs. glucose (5 mg/mL).

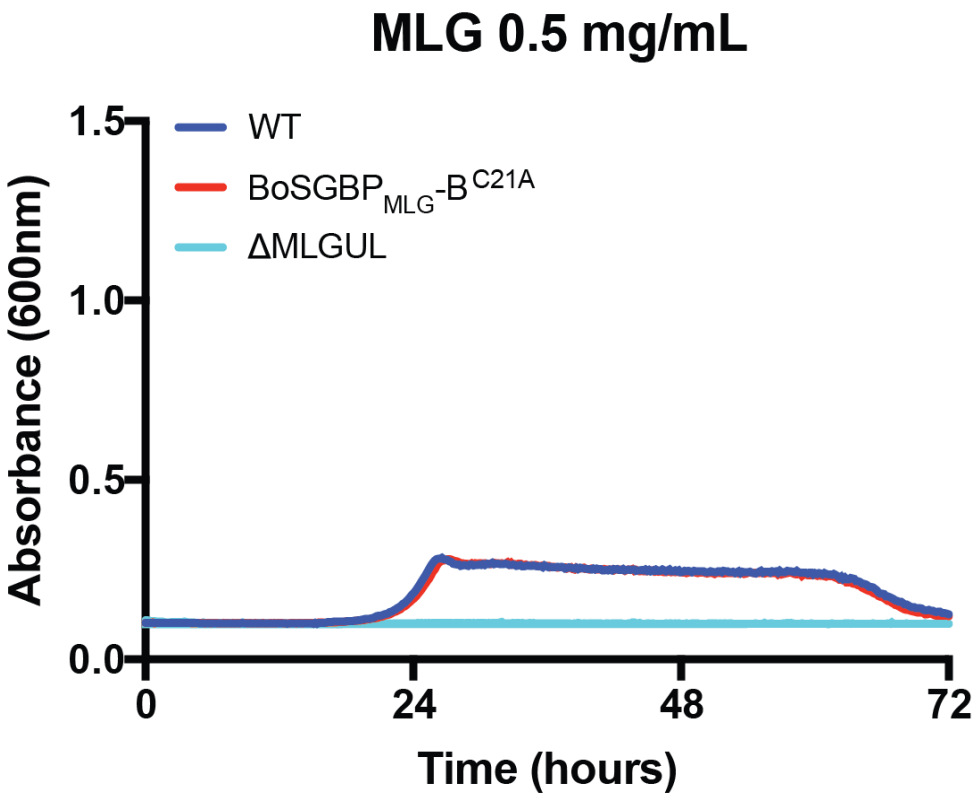

Figure S12. Average growth of *B. ovatus* on 0.5 mg/mL MLG. Limited (low maximum O.D.) or no growth of strains on 0.5 mg/mL MLG.

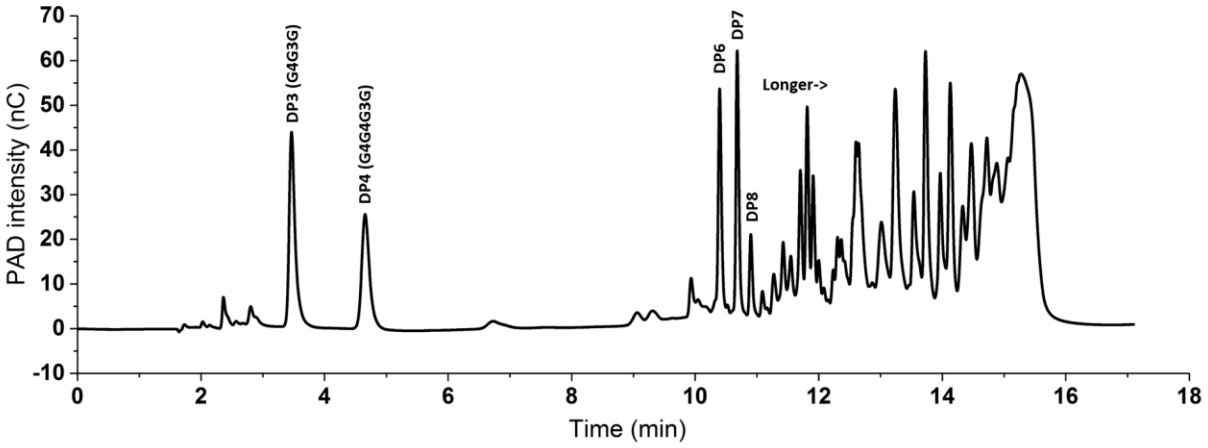

Figure S13. MLG partial digest HPLC profile. Controlled hydrolysis of MLG by recombinant $BoGH16_{MLG}$ produced a mixture containing predominantly oligosaccharides longer than the limit digest trisaccharide and tetrasaccharide.

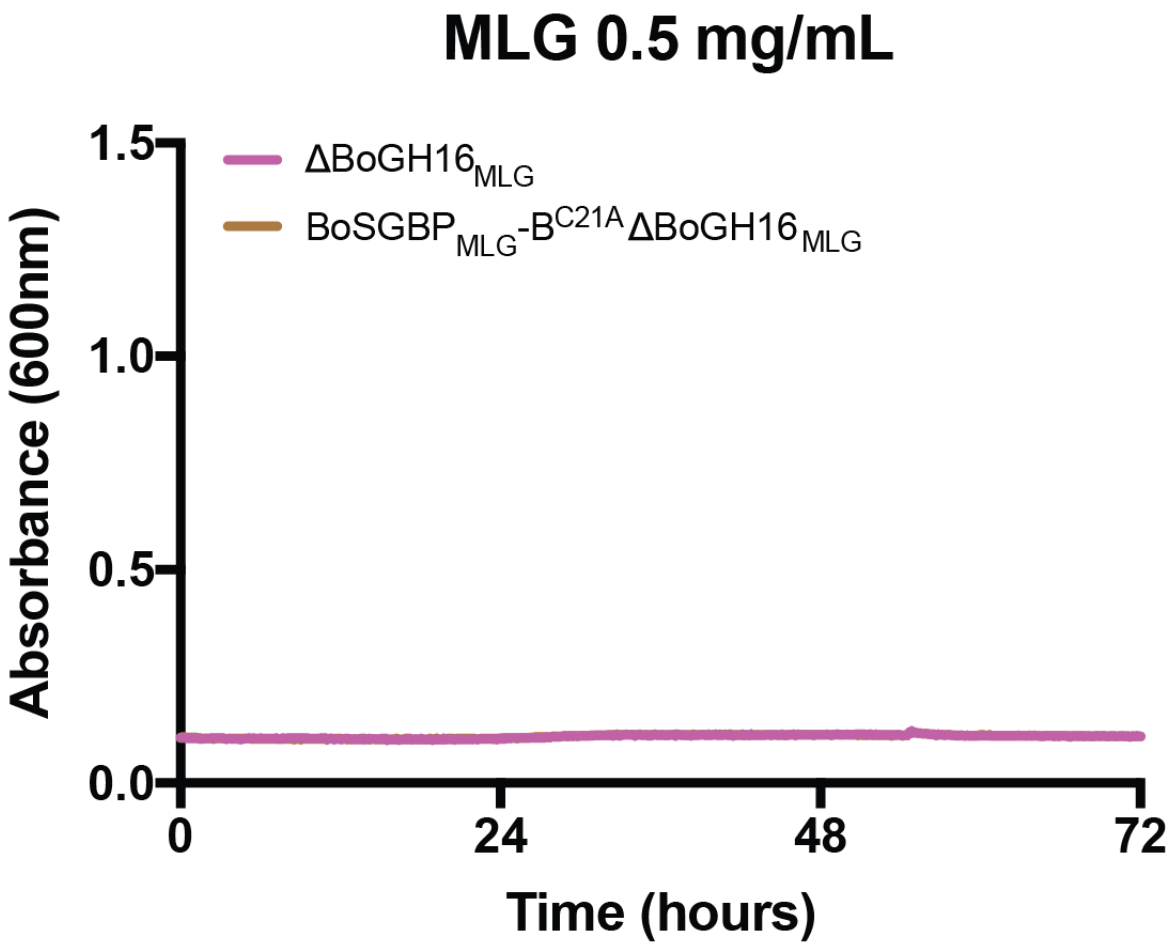

Figure S14. Average growth of *B. ovatus* strains lacking vanguard BoGH16 on 5 mg/mL MLG. BoGH16 is required for growth on MLG.

Table S1. Oligonucleotides used in this study.

Primer Name	Sequence (5'-3')	Use
SGBP-A F	GCGCGCCATATGGATGAATACATGGAAAAC	Cloning
SGBP-A R	GACGACCTCGAGTTAGTTTTCAGTATCCCA	Cloning
SGBP-A W77A F	CCGTAGTTGGTGGTGTTCGCACATCCCATCAGTTGTTG	Site-directed mutagenesis
SGBP-A W77A R	CAACAACTGATGGGATGTGCGAACACCACCAACTACGG	Site-directed mutagenesis
SGBP-A Y266A F	ATGAATTTCCGCGATAATCAGAGGCAGCTTCTTGTCCGAAACTAAATG	Site-directed mutagenesis
SGBP-A Y266A R	CATTTAGTTTCGGACAAGAAGCTGCCTCTGATTATCGCGGAAATTCAT	Site-directed mutagenesis
SGBP-A W350A F	GTAGGCCATGGTTCCGCCGAGTAGGCACCTGG	Site-directed mutagenesis
SGBP-A W350A R	CCAGGTGCCTACTCGGCGGAACCATGGCCTAC	Site-directed mutagenesis
SGBP-A W353A F	CCCTGTAGGCGCTGGTTCCCACGAGTAGGC	Site-directed mutagenesis
SGBP-A W353A R	GCCTACTCGTGGGAACCAGCGCCTACAGGG	Site-directed mutagenesis
SGBP-B F	GAAGAACATATGACCGAGGAAGAACCGTTC	Cloning
SGBP-B R	GACGACCTCGAGTTATTTCACGGTTACCAA	Cloning
SGBP-B W301A F	CACCGTCCGGCTTATCCGCCGAAACGTAATGGTGTC	Site-directed mutagenesis
SGBP-B W301A R	GACACCATTACGTTTCGGCGGATAAGCCGGACGGTG	Site-directed mutagenesis
SGBP-B Y341A F	CAAGCTGCATTTTATGAGCTTCGGCAGTAGGTTCTATGGAGTAG	Site-directed mutagenesis
SGBP-B Y341A R	CTACTCCATAGAACCTACTGCCGAAGCTCATAAAATGCAGCTTG	Site-directed mutagenesis
SGBP-B Y350A F	GCCAAGCCTGTCCAAGCGCCTGTGGCAAGCTG	Site-directed mutagenesis
SGBP-B Y350A R	CAGCTTGCCACAGGCGCTTGGACAGGCTTGGC	Site-directed mutagenesis
SGBP-B W351A F	CTTGCCAAGCCTGTCGCATAGCCTGTGGCAAGC	Site-directed mutagenesis
SGBP-B W351A R	GCTTGCCACAGGCTATGCGACAGGCTTGGCAAG	Site-directed mutagenesis
SGBP-B domainA R	TTATTACTCGACATCAGCCAACGGATTGAC	Cloning
SGBP-B domainB F	TACTGCCATATGGACCCTCAATCGAAAGAA	Cloning
SGBP-B domainB R	TAGTCGCTCGAGATTGGTTACTTTCACCAT	Cloning
SGBP-B domainC F	TAGTAGCATATGGCTTCCCTTGTCATTTCG	Cloning
SGBP-B domainC R	ATAATACTCGAGGGTAGATACGGTCACAGT	Cloning
SGBP-B domainD F	TCGACGCATATGGAAATAACGCTTTGGTCA	Cloning
GFP-fusion F	GTCAGCTAGCATGGTTAGCAAAGGTGAAGAA	Cloning
GFP-fusion R	GATGATGGATCCGCTGCCTTTATACAGTTCATC	Cloning

SGBP-A_GFP F	GACGACGGATCCATGGATGAATACATGGAAAAC	Cloning
SGBP-A_GFP R	GACGATCTCGAGTTAGTTTTCAGTATCCCACCA	Cloning
SGBP-B_GFP F	TATTATGGATCCATGACCGAGGAAGAACCGTTC	Cloning
SGBP-B_GFP R	GACGACCTCGAGTTATTTCACGGTTACCAAATC	Cloning
dMLGUL-A UpF	GAAGATAACATTCGAgtcgacGGTGGCCGCTAAGGTAGGCGAG	Deleting SGBP-A
dMLGUL-A UpR	GGATGATTGTTTAATAGGATATATCTTTTTAGAATTTCACATTTACATTAAAACCATAGCTTC	Deleting SGBP-A
dMLGUL-A DownF	GTGAAATTCTAAAAAGATATATCCTATTAAACAATCATCCATTATGAAAAAGATATATATTGCACTATTTGC	Deleting SGBP-A
dMLGUL-A DownR	GGCGGCCGCTCTAGAACTACATACGAGATTGATGCCGGAAATGGTCC	Deleting SGBP-A
dMLGUL-B UpF	GAAGATAACATTCGAgtcgacGGCTGATGAGTGCCACCAGTC	Deleting SGBP-B
dMLGUL-B UpR	GAATGATTTTTAAACTTACTTAGGAACAAATGGATGATTGTTTAATAGTTAGTTTTCAGTATCCC	Deleting SGBP-B
dMLGUL-B DownF	CTATTAAACAATCATCCATTTGTTCCTAAGTAAGTTTAAAAATCATTCATACCATAAGTATCTGTC	Deleting SGBP-B
dMLGUL-B DownR	GGCGGCCGCTCTAGAACTACTTGGAAGCCTCGGACAGCAG	Deleting SGBP-B
MLGUL-A* UpR	GGTATTCATGTTTTCCATGTATTCATCGCTGCAAGAAGCGAAAAACAGGGCAC	Replacing SGBP-A with SGBP-A*
MLGUL-A* F	AGCGATGAATACATGGAAAACATGAATACC	Replacing SGBP-A with SGBP-A*
MLGUL-A* R	TTAGTTTTCAGTATCCCACCACAGAAGGC	Replacing SGBP-A with SGBP-A*
MLGUL-A* DownF	GCCTTCTGTGGTGGGATACTGAAAACTAACTATTAAACAATCATCCATTATGAAAAAG	Replacing SGBP-A with SGBP-A*
dGH16 UpF	GAAAGAAGATAACATTCGAgtcgacGCTGCCGAACTGCTGAAAGAAGG	Deleting GH16
dGH16 UpR	GCATGTATATTTAAGATTCCGTTTTAGCATTTTAAAGGTTAAACGTAATATGTGC	Deleting GH16
dGH16 DownF2	CCTTTAAAATGCTAAAACGGAATCTTAAATATACATGCTATGAATATGGAAAAATGTAAGTATCTACTG	Deleting GH16
dGH16 DownR2	GGCGGCCGCTCTAGAACTACTGGCACGGCTACCATAAAGTGC	Deleting GH16
MLGUL-B C21A UpF	GAAAGAAGATAACATTCGAgtcgacGGCTGATGAGTGCCACCAGTC	Replacing SGBP-B with C21A allele
MLGUL-B C21A UpR	CTTCCTCGGTGCATGCAGTAAATGTGGAG	Replacing SGBP-B with C21A allele
MLGUL-B C21A DownF	CTCCACATTTACTGCATGCACCGAGGAAG	Replacing SGBP-B with C21A allele
MLGUL-B C21A DownR	GGCGGCCGCTCTAGAACTACTTGGAAGCCTCGGACAGCAG	Replacing SGBP-B with C21A allele
MLGUL TBDT qPCR F	CTATGTCTGCCCGTGCTGCTTAC	Probing TBDT transcription
MLGUL TBDT qPCR R	CCGGCTGCCAATCTTTCTTCT	Probing TBDT transcription
B ovatus 16s F	GGTAGTCCACACAGTAAACGATGAA	Normalizing transcription to 16s gene
B ovatus 16s F	CCCGTCAATTCCTTTGAGTTTC	Normalizing transcription to 16s gene

Table S2. Privateer validation results

Residue Name	Conformation	Average B-factor	RSCC	Diagnostic
$BoSGBP_{MLG}$-A MLG7 complex				
BGC-1	$^4C_1$	50.39	0.81	Ok
BGC-2	$^4C_1$	35.58	0.9	Ok
BGC-3	$^4C_1$	25.89	0.91	Ok
BGC-4	$^4C_1$	23.09	0.92	Ok
BGC-5	$^4C_1$	23.09	0.91	Ok
BGC-6	$^4C_1$	25.22	0.91	Ok
BGC-7	$^4C_1$	29.61	0.84	Ok
BGC-8	$^4C_1$	46.71	0.78	Ok
BGC-9	$^4C_1$	34.56	0.86	Ok
BGC-10	$^4C_1$	25.81	0.9	Ok
BGC-11	$^4C_1$	24.13	0.89	Ok
BGC-12	$^4C_1$	25.42	0.89	Ok
BGC-13	$^4C_1$	25.73	0.9	Ok
BGC-14	$^4C_1$	28.2	0.83	Ok
$BoSGBP_{MLG}$-B MLG7 complex				
BGC-1	$^4C_1$	105.22	0.36	Ok
BGC-2	$^4C_1$	65.6	0.78	Ok
BGC-3	$^4C_1$	58.94	0.79	Ok
BGC-4	$^4C_1$	62.14	0.73	Ok
BGC-5	$^4C_1$	63.7	0.71	Ok
BGC-6	$^4C_1$	74.5	0.63	Ok
BGC-7	$^4C_1$	94.15	0.34	Ok
$BoSGBP_{MLG}$-A cellohexaose complex				
BGC-1	$^4C_1$	60.1742	0.85	Ok
BGC-2	$^4C_1$	50.3745	0.93	Ok
BGC-3	$^4C_1$	46.6764	0.89	Ok
BGC-4	$^4C_1$	37.11	0.93	Ok
BGC-5	$^4C_1$	43.7827	0.87	Ok
BGC-6	$^4C_1$	58.41	0.79	Ok
BGC-7	$^4C_1$	46.1691	0.91	Ok
BGC-8	$^4C_1$	37.44	0.9	Ok
BGC-9	$^4C_1$	33.8336	0.93	Ok
BGC-10	$^4C_1$	39.5718	0.94	Ok

BGC-11	$^4C_1$	47.8636	0.83	Ok
BGC-12	$^4C_1$	67.5033	0.82	Ok
BGC-13	$^4C_1$	51.0927	0.9	Ok
BGC-14	$^4C_1$	43.9373	0.92	Ok
BGC-15	$^4C_1$	39.58	0.93	Ok
BGC-16	$^4C_1$	42.3864	0.95	Ok
BGC-17	$^4C_1$	49.8864	0.9	Ok
BGC-18	$^4C_1$	62.215	0.86	Ok
BGC-19	$^4C_1$	56.0618	0.89	Ok
BGC-20	$^4C_1$	51.0864	0.91	Ok
BGC-21	$^4C_1$	52.7482	0.91	Ok
BGC-22	$^4C_1$	56.2327	0.91	Ok
BGC-23	$^4C_1$	59.2864	0.89	Ok
BGC-24	$^4C_1$	65.1833	0.78	Ok
BGC-25	$^4C_1$	52.58	0.88	Ok
BGC-26	$^4C_1$	42.8782	0.92	Ok
BGC-27	$^4C_1$	37.2736	0.93	Ok
BGC-28	$^4C_1$	41.7655	0.89	Ok
BGC-29	$^4C_1$	41.3182	0.9	Ok
BGC-30	$^4C_1$	68.6325	0.8	Ok
BGC-31	$^4C_1$	57.5191	0.87	Ok
BGC-32	$^4C_1$	63.8582	0.83	Ok
BGC-33	$^4C_1$	56.5745	0.89	Ok
BGC-34	$^4C_1$	62.7182	0.88	Ok
BGC-35	$^4C_1$	70.1945	0.86	Ok
BGC-36	$^4C_1$	59.9958	0.85	Ok
BGC-37	$^4C_1$	47.8464	0.92	Ok
BGC-38	$^4C_1$	44.1164	0.92	Ok
BGC-39	$^4C_1$	38.3709	0.91	Ok
BGC-40	$^4C_1$	41.2236	0.94	Ok
BGC-41	$^4C_1$	45.3373	0.85	Ok
BGC-42	$^4C_1$	62.9917	0.83	Ok
BGC-43	$^4C_1$	54.4318	0.83	Ok
BGC-44	$^4C_1$	50.1036	0.84	Ok
BGC-45	$^4C_1$	50.4491	0.91	Ok
BGC-46	$^4C_1$	50.4491	0.91	Ok

BGC-47	$^4C_1$	55.8391	0.87	Ok
BGC-48	$^4C_1$	63.435	0.8	Ok
BGC-49	$^4C_1$	47.2318	0.91	Ok
BGC-50	$^4C_1$	43.8173	0.9	Ok
BGC-51	$^4C_1$	39.7791	0.92	Ok
BGC-52	$^4C_1$	43.8336	0.91	Ok
BGC-53	$^4C_1$	45.1427	0.89	Ok
BGC-54	$^4C_1$	58.5008	0.8	Ok
BGC-55	$^4C_1$	48.9773	0.9	Ok
BGC-56	$^4C_1$	40.7064	0.9	Ok
BGC-57	$^4C_1$	35.0218	0.91	Ok
BGC-58	$^4C_1$	41.4518	0.92	Ok
BGC-59	$^4C_1$	52.3018	0.87	Ok
$BoSGBP_{MLG}$-B cellohexaose complex				
BGC-1	$^4C_1$	47.1325	0.83	Ok
BGC-2	$^4C_1$	40.6309	0.88	Ok
BGC-3	$^4C_1$	40.0718	0.86	Ok
BGC-4	$^4C_1$	39.8464	0.86	Ok
BGC-5	$^4C_1$	46.6291	0.81	Ok
BGC-6	$^4C_1$	105.583	0.16	Ok
BGC-7	$^4C_1$	93.8809	0.54	Ok
BGC-8	$^4C_1$	86.8264	0.61	Ok
BGC-9	$^4C_1$	79.6155	0.73	Ok
BGC-10	$^4C_1$	80.81	0.67	Ok
BGC-11	$^4C_1$	110.487	0.25	Ok
BGC-12	$^4C_1$	93.9518	0.4	Ok
BGC-13	$^4C_1$	85.1655	0.55	Ok
BGC-14	$^4C_1$	77.7655	0.7	Ok
BGC-15	$^4C_1$	83.9127	0.62	Ok